Structural studies on *Desulfovibrio gigas* cytochrome c_3 by two-dimensional ^{1}H-nuclear-magnetic-resonance spectroscopy

Maria A. PIÇARRA-PEREIRA,* David L. TURNER,† Jean LEGALL‡ and António V. XAVIER*§

*Centro de Tecnologia Química e Biológica, Universidade Nova de Lisboa, Apartado 127, 2780 Oeiras, Portugal,
† Department of Chemistry, University of Southampton, Southampton S09 5NH, U.K., and ‡ Department of Biochemistry, University of Georgia, Athens, GA 30602, U.S.A.

Several aromatic amino acid residues and haem resonances in the fully reduced form of *Desulfovibrio gigas* cytochrome c_3 are assigned, using two-dimensional ^{1}H n.m.r., on the basis of the interactions between the protons of the aromatic amino acids and the haem protons as well as the intrahaem distances known from the X-ray structure [Kissinger (1989) Ph.D. Thesis, Washington State University]. The interhaem interactions observed in the n.m.r. spectra are in full agreement with the *D. gigas* X-ray structure and also with the n.m.r. data from *Desulfovibrio vulgaris* (Hildenborough) [Turner, Salgueiro, LeGall and Xavier (1992) Eur. J. Biochem. **210**, 931–936]. The good correlation between the calculated ring-current shifts and the observed chemical shifts strongly supports the present assignments. Observation of the two-dimensional nuclear-Overhauser-enhancement spectra of the protein in the reduced, intermediate and fully oxidized stages led to the ordering of the haems in terms of their midpoint redox potentials and their identification in the X-ray structure. The first haem to oxidize is haem I, followed by haems II, III and IV, numbered according to the Cys ligand positions in the amino acid sequences [Mathews (1985) Prog. Biophys. Mol. Biol. **54**, 1–56]. Although the haem core architecture is the same for the different *Desulfovibrio* cytochromes c_3, the order of redox potentials is different.

INTRODUCTION

Cytochrome c_3 from the sulphate-reducing bacterium *Desulfovibrio gigas* is a monomeric tetrahaem protein of low molecular mass (13.5 kDa) and low redox potential [1]. Each of the four haem prosthetic groups is covalently attached to a polypeptide chain of 112 amino acids by two thioether linkages provided by cysteine residues. The haem axial ligands are histidine residues.

The physiological role of cytochrome c_3 in *Desulfovibrio* remains unclear. It appears to be the electron-exchange partner of the periplasmic hydrogenase found in *Desulfovibrio* species and an essential component of the electron-transfer chain coupling the oxidation of molecular hydrogen by hydrogenase to sulphate reduction [2,3].

Although cytochrome c_3 has been found in all *Desulfovibrio* species examined so far, there is surprising variation in the amino acid sequences of protein from the different species. The sequences of six cytochrome c_3 molecules have now been determined and a sequence alignment has been proposed [4]. This alignment indicates that, of the 107–116 residues in the molecule, only 24 are strictly conserved. Of these, 16 are cysteine or histidine residues directly involved in binding of the haems. Both the X-ray structures of cytochrome c_3 from several species [5–8] and n.m.r. data [9,10] suggest that the relative orientation and arrangement of the four haems is conserved in spite of the low sequence similarity. There are aromatic residues close to the haems in all cytochrome c_3 molecules. It is noteworthy that one phenylalanine is similarly located and conserved in all six cytochromes [4]. This phenylalanine [5,7] is close to haems I and III in *D. baculatus* (Norway 4) (F34), *D. vulgaris* Miyazaki strain (F20) and *D. gigas* (F24), where the haems are numbered according to the Cys ligand positions in the amino acid sequences [11]. While phenylalanine and tyrosine residues are present in all six cytochrome c_3 molecules [4], tryptophan is found only in *D. gigas* (W68), *D. salexigens* (W41) and *D. desulfuricans* (El Algheila z) (W41). The X-ray structure shows that, in *D. gigas* [7], W68 is located close to the four haems, F12 close to the propionate groups of haems I and IV, Y46 close to haem I, and Y69 close to haem IV (Figure 1). The location of the aromatic amino acids for the cytochromes c_3 from *D. gigas*, *D. vulgaris* and *D. baculatus* are summarized in Table 1.

The Fe^{2+} ion in the reduced form of the protein is low-spin (electron spin quantum number $S = 0$) and the n.m.r. spectrum is that of a diamagnetic protein with a few resonances shifted by the strong ring currents of the porphyrins. In its oxidized form the Fe^{3+} ion has an electron spin quantum number $S = 1/2$, and the unpaired electron has a dramatic effect on the ^{1}H-n.m.r. spectrum of the protein, owing to its hyperfine interaction with neighbouring nuclei.

The electron distribution in a four-centre molecule leads to 16 microscopic redox states [12] which can be grouped in five macroscopic stages, connected by four one-electron steps. Each of the five stages (numbered 0–4, according to the number of oxidized haems) comprises a number of intermediate oxidation states which have the same number of oxidized haems. In the *D. gigas* cytochrome c_3, intermolecular electron exchange (between different stages) is slow on the n.m.r. time scale, but intramolecular exchange (within the same stage) is fast [1]. Consequently, a separate set of n.m.r. resonances is observed for the protons of the haems in each stage, their relative shifts being governed by the relative microscopic redox potentials of the haems [1,13].

Cytochrome c_3 is of considerable structural interest, not only because of the unusually low redox potentials of the haem iron atoms in the molecule, but also because of the complex network

Abbreviations used: 2D, two-dimensional; TOCSY, total correlation spectroscopy; Hi, *meso* protons at positions 5, 10, 15 and 20; Hi^1, thioether protons 3^1 and 8^1; Mi^1, methyl group protons 2^1, 7^1, 12^1 and 18^1; Mi^2, thioether methyl protons 3^2 and 8^2; NOESY, nuclear-Overhauser-enhancement spectroscopy; DSS, 4,4-dimethyl-4-silapentane sodium sulphonate.

§ To whom correspondence should be sent.

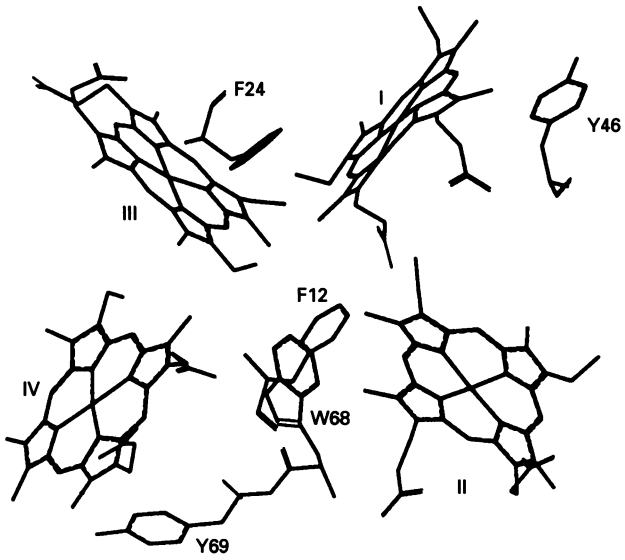

Figure 1 Orientation of the haems and selected aromatic residues from the X-ray co-ordinates of file dgc$_3$.pdb (see the Materials and methods section)

Haem numbering follows the Cys ligand positions in the amino acid sequence [11].

Table 1 Location of the aromatic amino acids with respect to the haems in cytochrome c_3 molecules from three *Desulfovibrio* species

Cytochrome c_3	Amino acid and position				Reference
Haem...	I	II	III	IV	
D. gigas	F12, F24, Y46, W68	W68	F24, W68	F12, Y69, W68	[7]
D. vulgaris (Miyazaki)	F20, Y43	H67, F76	F20, Y65, Y66		[6]
D. baculatus (Norway 4)	Y8, F34	F88	F34	F72, F88	[5]

of haem–haem co-operativities [1,14]. The main purpose of the present work was to complete the assignment of the proton resonances of the four haems and of the aromatic amino acids of cytochrome c_3 from *D. gigas*, in the reduced state, using two dimensional (2D) ^{1}H n.m.r. in conjunction with the calculated ring currents and the interproton distances known from the X-ray structure [7]. The assignment of the haem proton resonances in the reduced, intermediate and fully oxidized stages leads to the ordering of the four haems in terms of their midpoint redox potentials and to their identification in the X-ray structure. This assignment allows further comparative analysis of structure and function in this molecule. ^{1}H n.m.r. studies on the protein in the reduced, intermediate and fully oxidized stages have been used to identify the resonances of four methyl group protons which belong to four different haems in each of the five stages of oxidation.

MATERIALS AND METHODS

D. gigas (N.C.I.B. 9332) cytochrome c_3 was purified as previously described [15], dialysed against distilled, deionized water at 4 °C, freeze-dried twice from ^2H_2O (99.9 atom %) and dissolved in ^2H_2O (100 atom %) to a concentration of 2 mM. The pH was adjusted with NaO^{2}H and/or ^{2}HCl; pH values refer to meter readings uncorrected for the isotope effect.

Solutions of the fully reduced protein were obtained by adding 25 μg of hydrogenase purified from *D. gigas* [16] to 0.4 ml of the protein solution, under N_2, and then substituting H_2 for N_2. The sample was maintained under H_2 pressure. Samples were allowed to reoxidize by substituting N_2 for H_2 and gradually introducing small aliquots of air into the n.m.r. tube, with a Hamilton syringe, through serum caps.

The ^{1}H-n.m.r. spectra were obtained using a Bruker AMX-500 spectrometer equipped with a Bruker X32 computer. The data were collected at 298 K and with 1.3 s water presaturation, unless otherwise specified. Temperatures were adjusted with an Eurotherm temperature controller and a Haake thermostatic bath.

The total-correlation-spectroscopy (TOCSY) (50 ms mixing time) experiment was performed using the MLEV spinlock sequence [17,18]. The 2D nuclear-Overhauser-enhancement-spectroscopy (NOESY) [19] experiments were performed at 50, 200 and 400 ms mixing time with the fully reduced protein, and with a mixing time of 25 ms for the protein in intermediate stages of oxidation.

Chemical shifts are presented in p.p.m. relative to 4,4-dimethyl-4-silapentane sodium sulphonate (DSS), but formate was used as an internal reference.

The ring-current shifts were calculated from the crystal structure of cytochrome c_3 from *D. gigas* at a resolution of 0.25 nm [7] with the classical Johnson–Bovey model [20] using eight pairs of current loops to represent each haem, with the parameters obtained by Cross and Wright [21]. These shifts were corrected for the effect of the aromatic side chains [10].

Computer-graphics models were manipulated in a Silicon Graphics workstation using the Sybyl software; X-ray co-ordinates for cytochrome c_3 from *D. gigas* were kindly supplied by Dr. Larry C. Sieker [7].

RESULTS AND DISCUSSION

Resonance assignment in the reduced protein

Although the general features of the n.m.r. spectra of ferrocytochrome c_3 from *D. gigas* have been discussed [22,23], the proton resonances of the four haems and of the aromatic amino acids have not been assigned specifically.

In the protein from *D. vulgaris* (Hildenborough), specific assignments for the four haems were obtained by comparing the observed chemical shifts with calculated values for the ring current shifts which arise from other haems and aromatic residues [10]. Observation of both interhaem n.O.e.s and connectivities between aromatic and haem protons confirmed these assignments. The shape, number and relative intensity of the peaks observed in the NOESY spectra (Figures 2a and 2b) of ferrocytochrome c_3 from *D. gigas* indicate that several of the haem proton resonances overlap (Table 2), making the assignment more difficult. Thus a different strategy was followed in the n.m.r. studies of this protein, beginning with the identification of resonances whose assignment is obvious. The X-ray structure [7] shows that several of the aromatic amino acids of the protein are located quite close to the haems. In particular, W68 is close to protons of all four haems (Figure 1, and Tables 1 and 3). Therefore all possible aromatic-amino-acid proton resonances were identified, and the expected W68–haem interactions [7] were used to make the assignments listed in Table 3. Once the chemical shifts of a few protons from each haem were known, the remaining haem proton resonances could be identified by locating

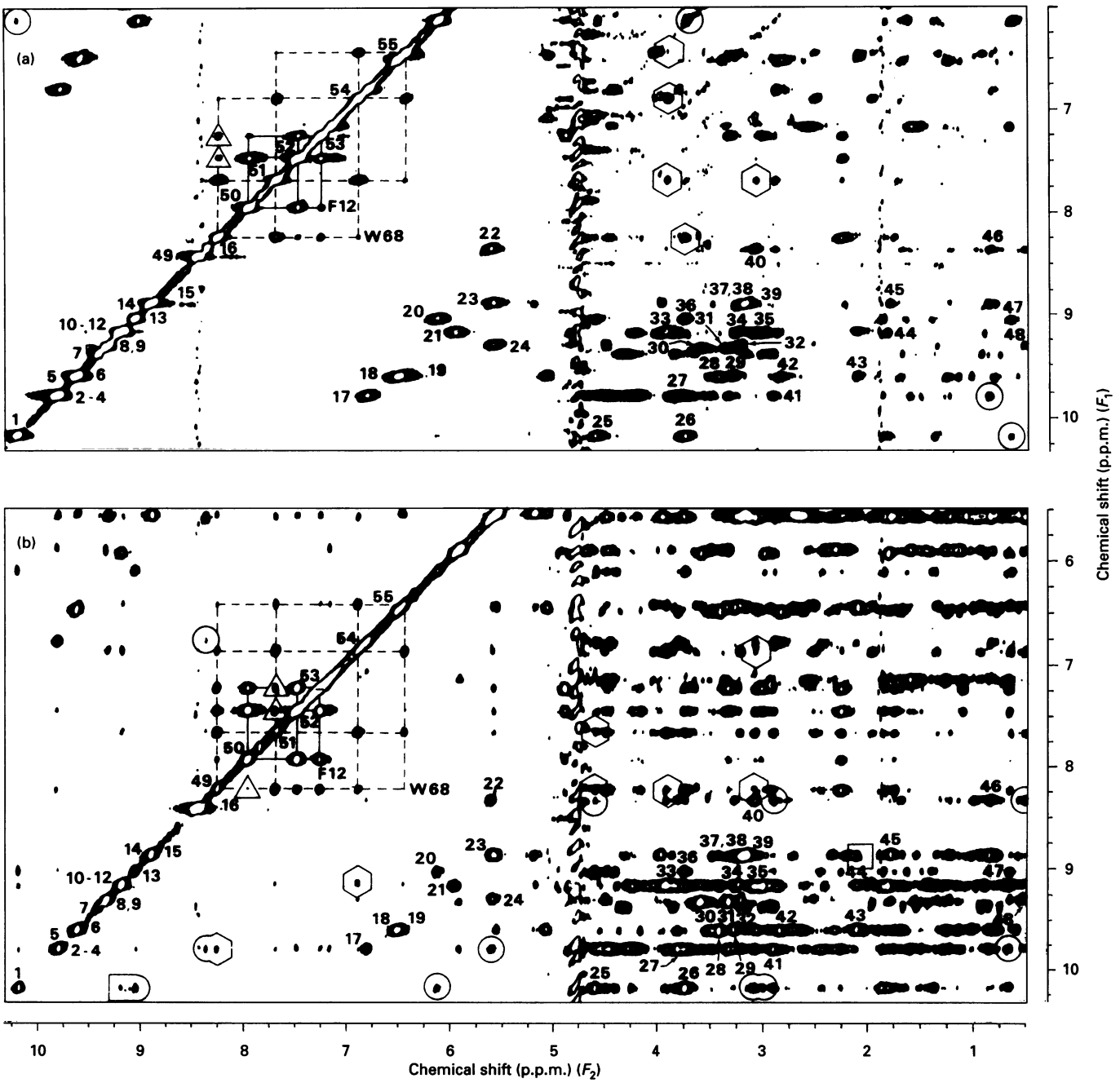

Figure 2 (a) NOESY ^{1}H-n.m.r. spectrum of ferrocytochrome c_3 from *D. gigas* (2 mM ^2H_2O, pH 9.74) and (b) the same, but with a mixing time of 400 ms

(**a**) The experiment was performed at 500 MHz and 298 K with 1.3 s water presaturation, a mixing time of 50 ms and 2048 (F_2) × 512 (F_1) data points. The spectrum was transformed using a cosine multiplication in F_2 and a shifted sine-bell multiplication in F_1 with zero-filling to 1024 data points in F_1. The Arabic numerals represent the several haem and amino acid resonances listed in Table 2. Because some of the resonances fall in crowded regions of the spectrum the *meso*-thioether, *meso*-methyl and *meso*-thioether methyl proton connectivities (numbered from 17 to 48) are labelled instead of the main diagonal resonance positions. Broken lines show the W68 connectivities, whereas continuous lines represent those of F12. Interhaem, tryptophan–phenylalanine and tryptophan–haem proton n.O.e.s are represented by open circles, triangles and hexagons, respectively. (**b**) The spectrum was transformed using a cosine multiplication in F_2 and a shifted sine-bell multiplication in F_1 with zero-filling to 1024 data points in F_1. The Arabic numerals represent the several haem and amino acid resonances listed in Table 2. Broken lines show the W68 connectivities, whereas continuous lines represent those of F12. Additional interhaem, intrahaem, tryptophan–phenylalanine and tryptophan–haem proton n.O.e.s are represented by open circles, squares, triangles and hexagons respectively.

the expected intrahaem connectivities. Finally, the interhaem n.O.e.s and the calculated ring-current shifts were used to confirm the proposed assignments.

The individual aromatic amino acids present in a protein can be identified in 2D ^{1}H-n.m.r. spectra [24] by their characteristic patterns of cross-peaks. Those of the tryptophan (W68) and of the phenylalanine (F12) are clearly observable in the 50 ms TOCSY spectrum (results not shown), which correlates nuclei belonging to the same spin system. The specific assignment of this phenylalanine was made by considering the interactions

Table 2 Chemical shifts (δ) of haem and aromatic amino acid proton resonances in reduced cytochrome c_3 from *D. gigas* (temperature 298 K; pH 9.74)

Resonance†	*meso* Proton	Chemical shift (δ) (p.p.m.)	Resonance†	Thioether proton	δ (p.p.m.)	Resonance†	Methyl proton	δ (p.p.m.)	Resonance†	Aromatic amino acid	δ (p.p.m.)
1	H20 (III)*	10.18	17	$H3^1$ (III)	6.82	25	$M2^1$ (III)	4.60	49	W68 (H-7)	8.26
2	H5 (III)	9.80	18	$H8^1$ (III)	6.51	26	$M18^1$ (III)	3.74	50	F12 (H-4)	7.98
3	H15 (IV)	9.80	19	$H3^1$ (I)	6.48	27	$M7^1$ (III)	3.81	51	W68 (H-6)	7.69
	H15 (I)	9.80	20	$H8^1$ (IV)	6.14	28	$M12^1$ (III)	3.42	52	F12 (H-3,5)	7.48
5	H10 (III)	9.60	21	$H3^1$ (IV)	5.96	29	$M7^1$ (I)	3.28	53	F12 (H-2,6)	7.25
6	H5(I)	9.58	22	$H8^1$ (I)	5.62	30	$M2^1$ (IV)	3.59	54	W68 (H-5)	6.90
7	H15 (II)	9.41	23	$H8^1$ (II)	5.60	31	$M18^1$ (IV)	3.33	55	W68 (H-4)	6.46
8	H5 (II)	9.32	24	$H3^1$ (II)	5.60	32	$M7^1$ (II)	3.22			
9	H20 (IV)	9.32				33	$M2^1$ (II)	3.93			
10	H5 (IV)	9.18	41	$M3^2$ (III)	2.90	34	$M18^1$ (II)	3.24			
11	H20 (II)	9.18	42	$M8^2$ (III)	2.84	35	$M7^1$ (IV)	3.00			
12	H15 (III)	9.18	43	$M3^2$ (I)	2.10	36	$M12^1$ (IV)	3.75			
13	H10 (IV)	9.06	44	$M3^2$ (IV)	1.82	37	$M2^1$ (I)	3.20			
14	H20 (I)	8.90	45	$M8^2$ (II)	1.80	38	$M18^1$ (I)	3.20			
15	H10 (II)	8.88	46	$M8^2$ (I)	0.84	39	$M12^1$ (II)	3.15			
16	H10 (I)	8.36	47	$M8^2$ (IV)	0.66	40	$M12^1$ (I)	3.07			
			48	$M3^2$ (II)	0.56						

* The Roman numerals in parentheses represent the haem numbers following the Cys ligand positions in the amino acid sequence [11].

† These numbers refer to peaks in Figure 2. Because some of the resonances fall in crowded regions of the spectrum the *meso*-thioether, *meso*-methyl and *meso*-thioether methyl proton connectivities (numbered from 17 to 48) are labelled instead of the positions on the main diagonal.

Table 3 Intensities of the W68–haem proton n.O.e.s versus the internuclear distances taken from the X-ray structure [7]

The intensities are: S (strong), M (medium), W (weak), VW (very weak), O (obscured by other peaks) and – (not observable).

Connectivities	Distance (nm)	Intensity of the connectivity		
	Mixing time (ms)...	50	200	400
W68 (H-7)–$M12^1$ (IV)	0.3312	S	S	S
W68 (H-5)–$M2^1$ (II)	0.3657	S	S	S
W68 (H-6)–$M12^1$ (IV)	0.4141	VW	M	S
W68 (H-6)–$M12^1$ (I)	0.4338	S	S	S
W68 (H-6)–$M2^1$ (II)	0.5327	S	S	S
W68 (H-5)–$M12^1$ (I)	0.5337	VW	VW	W
W68 (H-4)–$M2^1$ (II)	0.5349	W	O	O
W68 (H-7)–H15 (IV)	0.5594	–	VW	VW
W68 (H-5)–H20 (II)	0.5722	–	VW	W
W68 (H-6)–$M2^1$ (III)	0.5929	–	VW	VW
W68 (H-7)–$M12^1$ (I)	0.6328	–	VW	W
W68 (H-7)–$M2^1$ (III)	0.6619	–	VW	W
W68 (H-7)–$M2^1$ (II)	0.7655	–	W	M

between W68 and F12, observable in the NOESY spectra (Figures 2a and 2b), since the X-ray structure [7] shows that the only aromatic residue close to W68 in F12. In fact, the distances between H-7 of the W68 side chain and H-2,6 and H-3,5 of the F12 side chain are 0.290 nm and 0.295 nm respectively. The NOESY spectrum at a mixing time of 50 ms (Figure 2a) shows the short-range interactions (less than about 0.55 nm) [9,10]. Longer-range interactions require longer mixing times (200 and 400 ms). For the sake of clarity, only a few of the aromatic amino acid, and intra- and inter-haem interactions are indicated in Figures 2(a) and 2(b) (compare with Tables 3 and 4). The 50 ms NOESY spectrum (Figure 2a) shows a weak cross-peak between a proton resonance of W68 and a proton resonance of F12 at 7.48 p.p.m., and a slightly stronger cross-peak between the same proton of W68 and another proton resonance of F12 at 7.25 p.p.m. Thus the W68 resonance belongs to H-7 and the F12 resonances to H-3,5 (7.48 p.p.m.) and H-2,6 (7.25 p.p.m.). The NOESY and TOCSY spectra show cross-peaks between H-2,6 (7.25 p.p.m.) and H-3,5 (7.48 p.p.m.) of F12 and a one-proton resonance of this same residue which is assigned to H-4 (7.98 p.p.m.). A larger number of interactions between the protons of W68 and F12 is observable in the 400 ms NOESY spectrum (Figure 2b), and the relative intensities of the cross-peaks agree with the internuclear distances known from X-ray data [7]. The chemical shifts of the W68 and F12 protons are listed in Table 2.

A diagram of haem *c* is shown in Figure 1 of the preceding paper [32], numbered according to the IUPAC–IUB nomenclature [25]. In the spectrum of the reduced protein (Figure 2a) the *meso* protons give rise to 16 one-proton intensity signals in the region of 8–11 p.p.m. The eight thioether proton peaks appear between 5 and 7 p.p.m.; 16 signals of three-proton intensity, corresponding to the haem methyl groups, are observed in the region 3–5 p.p.m., and the thioether methyl protons appear between 0.5 and 3 p.p.m. The interactions between each thioether proton and its *vicinal* thioether methyl proton are observable in a 50 ms TOCSY spectrum (results not shown).

Table 3 lists the interactions between W68 and haem protons and compares the intensities of the cross-peaks observed at 50 ms (Figure 2a), 200 ms (spectrum not shown) and 400 ms (Figure 2b) with the distances taken from the crystal structure [7]. Observation of the W68–haem proton-resonance connectivities leads directly to the specific cross-assignment of several signals to individual haems in the X-ray structure: *meso* protons $H20_{II}$ (9.18 p.p.m.) and $H15_{IV}$ (9.80 p.p.m.), and methyl protons $M12^1{}_{I}$ (3.07 p.p.m.) and $M2^1{}_{II}$ (3.93 p.p.m.). Methyl protons $M12^1{}_{IV}$ (3.75 p.p.m.) and $M2^1{}_{III}$ (4.60 p.p.m.) were assigned by comparing their distances to protons H-7 and H-6 of W68 with the intensities of the respective interactions (Table 3).

To identify the remaining resonances of each haem, the structure of haem *c* (Figure 1 of [32]) must be considered. For example, in haem II, the assignment of H20 and $M2^1$ leads to that of $M18^1$ (3.24 p.p.m.) (Figure 2a). The n.O.e. between $M2^1$ and *meso* proton H5 of the same haem is shown in Figure 2(b). The short-range connectivities between H5 (9.32 p.p.m.) and $H3^1$, H5 and $M3^2$ become evident in Figure 2(a). The spectra indicate that the chemical shift of $M7^1$ is 3.22 p.p.m., and consequently H10 resonates at 8.88 p.p.m. Indeed, although the connectivity between $M7^1$ and H10 is obscured by other resonances, the n.O.e.s between H10 and $H8^1$ and H10 and $M8^2$ are easy to identify (Figure 2a), and the interactions between $M7^1$ and $H8^1$ and $M7^1$ and $H3^1$ are observable in both spectra (Figures 2a and 2b). The *meso* proton at 9.41 p.p.m. is H15. In fact, it interacts with the propionate protons at 3.17–4.34 p.p.m. (Figure 2a), and an n.O.e. is observed between H15 and $M18^1$. Only $M12^1$ remains to be assigned. Figure 2(b) shows an n.O.e. between H15 and a resonance at 3.15 p.p.m., which is, therefore, assigned to $M12^1$.

A similar approach was used for the specific assignment of the other haem protons. Table 2 lists all the resonances and their respective chemical shifts, and Table 4 lists the interhaem

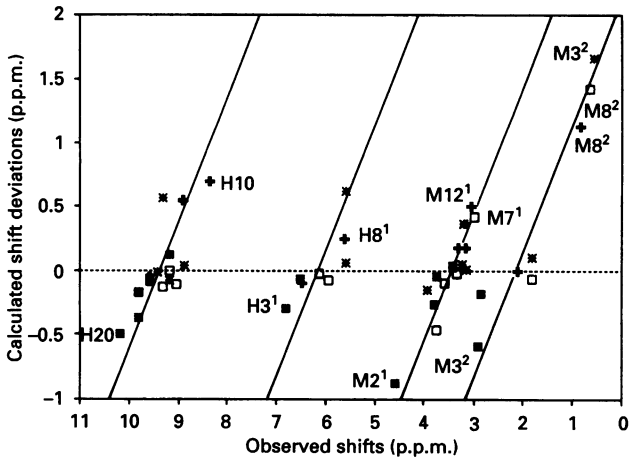

Figure 3 Plot of the calculated ring-current shifts versus the observed chemical shifts (Table 2) for all the protons of the four haems of cytochrome c_3 from *D. gigas*

The several protons are represented by the symbols: Haem I (+), Haem II (*), Haem III (■) and Haem IV (□). The lines show the best fits with a unit slope for each set of protons. The calculated ring-current shifts were obtained as described in the Materials and methods section. The starting chemical shifts for all the haem protons, from which the shift deviations were obtained, were calculated in the same way, using the crystal structure and the observed chemical-shift data for cytochrome *c* [10].

Table 4 Intensities of the interhaem n.O.e.s versus the internuclear distances taken from the X-ray structure [7]

The intensities are: S (strong), M (medium), W (weak), VW (very weak), O (obscured by other peaks) and – (not observable).

Connectivity	Distance (nm)	Intensity of the connectivity, Mixing time (ms) ... 50	200	400
H10 (IV)–$M2^1$ (III)	0.3359	S	S	S
H5 (III)–$M8^2$ (I)	0.3740	S	S	S
$M2^1$ (III)–$H8^1$ (IV)	0.3973	S	S	S
H10 (I)–$M3^2$ (III)	0.4434	O	S	S
H20 (III)–$H8^1$ (IV)	0.4591	W	W	W
$M7^1$ (III)–$H8^1$ (I)	0.4602	–	VW	W
H10 (I)–$M3^2$ (II)	0.4777	O	S	M
H20 (III)–$M8^2$ (IV)	0.5057	W	S	M
H20 (III)–H10 (IV)	0.5280	–	W	W
$M12^1$ (I)–$H3^1$ (II)	0.5329	M	S	S
$M12^1$ (I)–$H3^1$ (III)	0.5369	–	VW	W
$M18^1$ (III)–$H8^1$ (IV)	0.5434	O	O	O
H10 (I)–$H3^1$ (III)	0.5435	–	–	VW
H10 (I)–$M2^1$ (II)	0.5453	–	VW	W
$M12^1$ (IV)–$H3^1$ (III)	0.5486	–	VW	VW
H10 (I)–$H3^1$ (II)	0.5491	O	O	O
H10 (I)–H5 (III)	0.5528	–	–	VW
H10 (IV)–$M3^2$ (III)	0.5537	–	VW	W
H5 (III)–$M8^2$ (IV)	0.5903	–	VW	M
$M2^1$ (II)–$H3^1$ (I)	0.6133	–	O	O
H15 (I)–$M3^2$ (II)	0.6378	–	VW	W
H5 (III)–$M2^1$ (II)	0.6564	O	O	O
H20 (III)–$M12^1$ (IV)	0.6580	O	O	O
H5 (III)–$M12^1$ (I)	0.6593	–	O	O
H10 (I)–$M7^1$ (III)	0.6622	–	–	VW
H10 (I)–$M2^1$ (III)	0.6980	–	–	VW
H20 (II)–$M7^1$ (III)	0.7083	O	O	O
H15 (I)–$H3^1$ (II)	0.7290	–	–	VW
H5 (III)–$M7^1$ (I)	0.7304	O	O	O
H20 (III)–$M7^1$ (IV)	0.7375	–	VW	VW
H20 (III)–$M12^1$ (I)	0.7915	–	W	M
H20 (II)–$M12^1$ (I)	0.7989	O	O	O
H5 (II)–$M12^1$ (I)	0.8012	–	–	VW
H5 (III)–$M12^1$ (IV)	0.8122	O	O	O

connections and compares the intensities of the cross-peaks observed at 50 ms (Figure 2a), 200 ms (spectrum not shown) and 400 ms (Figure 2b), with the distances taken from the crystal structure [7]. The ordering of the cross-peak intensities at each mixing time with respect to the internuclear distances is not monotonic as a result of variable spin-diffusion effects [26]. The interhaem n.O.e.s observed are in perfect agreement with the known three-dimensional structure [7], confirming that the above assignments are correct and that the arrangement of the haems in solution and in the crystal structure is similar.

A plot of the ring-current-shift deviations for the haem protons, calculated as described in Materials and methods section, versus the observed chemical shifts (see Table 2) is shown in Figure 3. The values of the shifts in the absence of any ring-current contribution (*meso* 9.36 p.p.m., thioether 6.13 p.p.m., methyl 3.48 p.p.m. and thioether methyl protons 2.12 p.p.m.) were obtained by correcting the observed shifts in the horse cytochrome *c* spectrum [10]. The graph shows a good correlation, which strongly supports the previous assignment. Indeed, the calculation predicts that the *meso* proton with the largest downfield shift is $H20_{III}$, which agrees with the experimental data in the sense that this *meso* proton is connected through n.O.e.s to the thioether $H3^1$, the methyl group $M2^1$ and the thioether methyl group protons $M3^2$, all displaying the largest downfield shifts. Similarly, *meso* proton $H10_I$, the thioether $H8^1{}_I$, the methyl group $M12^1{}_I$ and the thioether methyl group protons $M8^2{}_I$ are all strongly shifted upfield. The calculated and the observed values for the shifts (Figure 3) show that the thioether methyl group $M3^2{}_{II}$ and the methyl group $M7^1{}_{IV}$ and the thioether methyl group protons $M8^2{}_{IV}$ have large upfield shifts.

Paramagnetic shifts

As stated above, since the interconversion between oxidation states belonging to the same stage (intramolecular electron exchange) is fast on the n.m.r. time scale ($> 10^5\ s^{-1}$) and the interconversion between states belonging to different stages

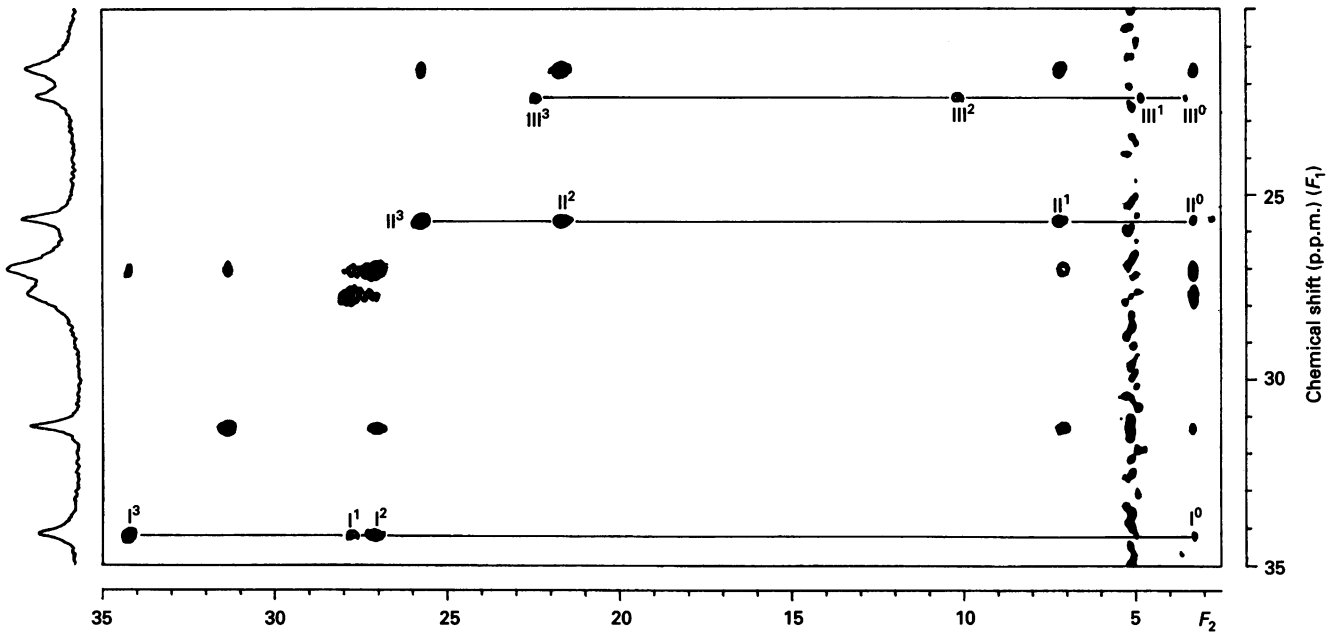

Figure 4 NOESY ^{1}H-n.m.r. spectrum of cytochrome c_3 from *D. gigas* (2 mM in ^2H_2O) in an intermediate stage of oxidation

The experiment was performed at 500 MHz and 276 K with 1.8 s water presaturation, a mixing time of 25 ms and 2048 (F_2) × 512 (F_1) data points. The spectrum was transformed using a Gaussian apodization (lb = −15 Hz, gb = 0.12) in F_2 and a shifted sine-bell multiplication in F_1 with zero-filling to 1024 data points in F_1. The cross-peaks connecting the chemical shifts of three methyl groups in stages 0–2 to their shifts in stage 3 have been labelled. The Roman numerals I–III identify the haems in the protein structure which, coincidentally, is also the order of their redox potentials starting from the lowest one. The superscripts (0–3) indicate the particular oxidation stage.

Table 5 Chemical shifts (δ) of one methyl group from each haem in the five oxidation states, and the corresponding oxidation fractions, x_i

Three of the methyl groups are identified, and the particular haem each one belongs to is specified by a subscript Roman numeral. The assignment of the methyls from haems I and IV are ambiguous: the shifts of $M18^1_I$ and $M2^1_I$ are identical in the reduced form, and the shift differences for haem IV in stages 0–3 are too small to monitor, so the assignment is made in the fully oxidized form.

	δ (p.p.m.)				x_i			
Stage	$M18^1_I/M2^1_I$	$M7^1_{II}$	$M12^1_{III}$	$M18^1_{IV}/M2^1_{IV}$	$M18^1_I/M2^1_I$	$M7^1_{II}$	$M12^1_{III}$	$M18^1_{IV}/M2^1_{IV}$
0	3.22/3.22	3.24	3.5	3.59/3.33	0.0	0.0	0.0	0.0
1	27.67	7.18	4.80	–	0.786	0.173	0.068	–
2	27.10	21.59	10.13	–	0.768	0.808	0.339	–
3	34.16	25.66	22.34	5.4	0.995	0.987	0.960	0.065
4	34.32	25.96	23.13	32.88	1.0	1.0	1.0	1.0

(intermolecular exchange) is slow [1], a separate set of signals is observed for the haem protons in each of the five different stages. Thus at each stage their chemical shifts depend on the ratio between the molar fractions of the states in which the haem considered is oxidized and the states in which the same haem is reduced.

In earlier work, several of the haem-methyl-group resonances were monitored through the different oxidation stages using several series of selective one-dimensional saturation-transfer experiments at different solution redox potentials [1]. The selective irradiation required for one-dimensional saturation-transfer experiments is difficult to achieve in crowded regions of the spectrum, but that selectivity is not necessary in 2D ^{1}H n.m.r., and a single experiment provides the information of many saturation-transfer experiments [27–29].

With the assignment of the haem proton resonances of ferrocytochrome c_3 from *D. gigas* completed, observation of intermediate stages of oxidation allows the ordering of the haems in terms of their midpoint redox potentials and their identification in the X-ray structure Recently, the four haems of *D. vulgaris* (Hildenborough) cytochrome c_3 were cross-assigned according to their redox potentials in this way [28]. Each individual haem resonance in an intermediate stage of oxidation is cross-assigned to its position in lower stages of oxidation and finally to the fully reduced stage. The result is a self-consistent network of cross-peaks leading to the unambiguous assignment of each haem group in the crystal structure. The NOESY data for cytochrome c_3 from *D. gigas* in a solution poised at a redox potential at which oxidation stages 0–3 co-exist are shown in Figure 4. The peaks corresponding to three methyl groups belonging to three different haems are indicated. To minimize contributions from extrinsic paramagnetic shifts (the result of interhaem pseudocontact shifts [1]), the methyl groups chosen point towards the protein surface and are, therefore, far from the other haems. Table 5 lists the

chemical shifts of the three methyl groups (stages 0–4) together with those of a fourth methyl group belonging to the last haem to oxidize, in the five redox stages. Cross-assignment from stage 3 to the fully oxidized form was achieved by using the NOESY spectrum of a solution in which stages 3 and 4 were the dominant forms (results not shown). This spectrum also revealed exchange peaks for methyls of the fourth haem, which remains almost fully reduced in stages 0–3. The small shifts of these methyls in the early stages of reoxidation make it difficult to follow them back to their positions in the fully reduced protein, but a methyl–methyl n.O.e. observed in the fully oxidized form is sufficient to assign the peak at 32.88 p.p.m to either $M18^1_{IV}$ or $M2^1_{IV}$. According to the X-ray data [7], both these methyls also point towards the protein surface.

Table 5 also shows the degrees of oxidation calculated for each haem from the ratio of the paramagnetic shifts of the methyl groups at each stage to their total shifts in the fully oxidized protein. These results are in agreement with earlier work [1,30], and it is now possible unequivocally to cross-assign the previously calculated midpoint redox potentials to the individual haems in the structure (Table 5). Haem I has the most negative redox potential (−340 mV), followed by haems II (−285 mV), III (−280 mV) and IV (−205 mV) [30].

Conclusions

The agreement between the n.m.r. (the present study) and the crystallographic data [7] shows that the above assignment is correct and that the arrangement of the haems in solution and in the crystal structure is similar. Recent n.m.r. studies of cytochromes c_3 from *D. vulgaris* (Hildenborough) [9] and *D. baculatus* (Norway 4) [10] and X-ray data for *D. gigas* [6] and *D. vulgaris* [7] show that the arrangement and orientation of the haems is maintained in all these proteins. The pattern of n.O.e.s observed between protons belonging to different haems are identical for cytochrome c_3 molecules which differ as much as 70% in their primary sequence. It is remarkable how such relatively small molecules stabilize the four paramagnetic centres, maintaining a similar basic architecture.

However, these cytochromes c_3 differ in the order of redox potentials [28,31]. 2D ^{1}H-n.m.r. redox studies on cytochrome c_3 from *D. vulgaris* (Hildenborough) show that the first haem to oxidize is haem III, followed by haems II, I and IV [28], and the assignment of the midpoint redox potentials of *D. baculatus* (Norway 4) using e.p.r. spectroscopy of single crystals indicates that haem II oxidizes first, followed by haems I, IV and III [31]. The e.p.r. results of *D. baculatus* (Norway 4) are compatible with the cross-assignment obtained by n.m.r. studies (the preceding paper [32]). Studies on the influence of the polypeptide chain in controlling the observed differences, as well as their mechanistic implications, are now in progress.

Received 18 January 1993/13 May 1993; accepted 18 May 1993

We thank Dr. Larry C. Sieker for making available the co-ordinates for the X-ray crystal structure of *D. gigas*, and Isabel Pacheco and Fernando Matos for their technical assistance. This research was partially supported by National Institutes of Health grant GM 34903 (J. LeG.)

REFERENCES

1 Santos, H., Moura, J. J. G., Moura, I., LeGall, J. and Xavier, A. V. (1984) Eur. J. Biochem. **141**, 283–296
2 Odom, J. M. and Peck, H. D., Jr. (1984) Annu. Rev. Microbiol. **38**, 551–592
3 LeGall, J. and Fauque, G. (1988) in Biology of Anaerobic Microorganisms (Zehnder, A. J. B., ed.), pp. 587–639, John Wiley and Sons, New York
4 Higuchi, Y., Kusunoki, M., Yasuoka, N., Kakudo, M. and Yagi, T. (1981) J. Biochem. (Tokyo), **90**, 1715–1723
5 Pierrot, M., Haser, R., Frey, M., Payan, F. and Astier, J. P. (1982) J. Biol. Chem. **257**, 14341–14348
6 Higuchi, Y., Kusunoki, M., Matsuura, Y., Yasuoka, N. and Kakudo, M. (1984) J. Mol. Biol. **172**, 109–139
7 Kissinger, C. (1989) Ph.D. Thesis, Washington State University, Seattle
8 Morimoto, Y., Tani, T., Okumura, H., Higuchi, Y. and Yasuoka, N. (1991) J. Biochem. (Tokyo) **110**, 532–540
9 Coutinho, I. B., Turner, D. L., LeGall, J. and Xavier, A. V. (1992) Eur. J. Biochem. **209**, 329–333
10 Turner, D. L., Salgueiro, C. A., LeGall, J. and Xavier, A. V. (1992) Eur. J. Biochem. **210**, 931–936
11 Mathews, F. S. (1985) Prog. Biophys. Mol. Biol. **45**, 1–56
12 Palmer, G. and Olson, J. S. (1980) in Molybdenum and Molybdenum-Containing Enzymes (Coughlan, M., ed.), chapter 5, Pergamon Press, New York
13 Fan, K., Akutsu, H., Kyogoku, Y. and Niki, K. (1990) Biochemistry **29**, 2257–2263
14 Xavier, A. V. (1986) J. Inorg. Biochem. **28**, 239–243
15 LeGall, J., Mazza, G. and Dragoni, N. (1965) Biochim. Biophys. Acta **99**, 385–387
16 LeGall, J., Ljungdahl, P., Moura, I., Peck, H. D., Jr., Xavier, A. V., Moura, J. J. G., Teixeira, M., Huynh, B. H. and DerVartanian, D. V. (1982) Biochem. Biophys. Res. Commun. **106**, 610–616
17 Braunschweiler, L. and Ernst, R. R. (1983) J. Magn. Reson. **53**, 521–528
18 Bax, A. and Davis, D. G. (1985) J. Magn. Reson. **65**, 355–360
19 Jeener, J., Meier, B. H., Bachmann, P. and Ernst, R. R. (1979) J. Chem. Phys. **71**, 4546–4553
20 Johnson, C. E. and Bovey, F. A. (1958) J. Chem. Phys. **29**, 1012–1014
21 Cross, K. J. and Wright, P. E. (1985) J. Magn. Reson. **64**, 220–231
22 McDonald, C. C., Phillips, W. D. and LeGall, J. (1974) Biochemistry **13**, 1952–1959
23 Moura, J. J. G., Xavier, A. V., Cookson, D. J., Moore, G. R. and Williams, R. J. P. (1977) FEBS Lett. **81**, 275–280
24 Wüthrich, K. (1986) NMR of Proteins and Nucleic Acids, pp. 135–146, John Wiley and Sons, New York
25 Moss, G. P. (1988) Eur. J. Biochem. **178**, 277–328
26 Wüthrich, K. (1986) NMR of Proteins and Nucleic Acids, pp. 97–102, John Wiley and Sons, New York
27 Santos, H., Turner, D. L., LeGall, J. and Xavier, A. V. (1984) J. Magn. Reson. **59**, 177–180
28 Salgueiro, C. A., Turner, D. L., Santos, H., LeGall, J. and Xavier, A. V. (1992) FEBS Lett. **314**, 155–158
29 Xavier, A. V., Turner, D. L. and Santos, H. (1993) Methods Enzymol. **227**, in the press
30 Colleta, M., Catarino, T., LeGall, J. and Xavier, A. V. (1991) Eur. J. Biochem. **202**, 1101–1106
31 Guigliarelli, B., Bertrand, P., More, C., Haser, R. and Gayda, J.-P. (1990) J. Mol. Biol. **216**, 161–166
32 Coutinho, I. B., Turner, D. L., LeGall, J. and Xavier, A. V. (1993) Biochem. J. **294**, 899–908